IEEE Access
Multidisciplinary | Rapid Review | Open Access Journal

Received 10 December 2022, accepted 22 December 2022, date of publication 26 December 2022,
date of current version 5 January 2023.

Digital Object Identifier 10.1109/ACCESS.2022.3232282

RESEARCH ARTICLE

Optimal Scheduling and Cost-Benefit Analysis of Lithium-Ion Batteries Based on Battery State of Health

MOHAMMAD AMINI, MOHAMMAD HASSAN NAZARI, AND SEYED HOSSEIN HOSSEINIAN
Department of Electrical Engineering, Amirkabir University of Technology, Tehran 1591634311, Iran
Corresponding author: Seyed Hossein Hosseinian (hosseinian.aut@gmail.com)

ABSTRACT This paper presents a novel battery degradation cost (BDC) model for lithium-ion batteries (LIBs) based on accurately estimating the battery lifetime. For this purpose, a linear cycle counting algorithm is devised to estimate the battery cycle aging. In this algorithm, the local maximum and minimum values of the profile of the battery state of charge are identified by the proposed linear formulations. Then, the battery cycle aging due to the complete and incomplete cycles is determined. In this step, the battery cycle aging during an incomplete cycle is calculated by converting it to two complete cycles. After that, the calendar aging process of the LIB is linearly formulated based on the semi-empirical model to estimate the BDC accurately. After linearizing the LIB degradation process, a mechanism for computing the BDC during the scheduling horizon is designed by modeling the BDC as a series of equal payments over the LIB lifetime. In order to incorporate the BDC in the battery energy management problem, an iterative algorithm is presented for efficiently calculating the BDC associated with the adopted charging/discharging strategy. The numerical simulation results indicate that integrating the battery degradation process into the battery scheduling problem can reduce the amount of the battery capacity fading by 32.81%, as well as increase the profit of battery owners by 1.21%. Moreover, the conducted analyses highlight the importance of considering the LIB calendar aging process in determining the optimal LIB capacity.

INDEX TERMS Battery degradation cost (BDC), cycle aging process, calendar aging process, battery scheduling problem, wind energy.

NOMENCLATURE

A. INDICES AND SUPERSCRIPTS

cal	Superscript for battery calendar aging.
ch	Superscript for battery charging state.
cyc	Superscript for battery cycle aging.
dch	Superscript for battery discharging state.
h, t	Index for time interval.
n	Index for depth of discharge (DOD).
Ω^h	Set of time intervals.

B. PARAMETERS

C^E	Battery energy rating investment cost.
C^n	Battery installation cost.
C^P	Battery power rating investment cost.
E^{ins}	Battery initial energy capacity.
IC	Battery investment cost.
N^{fail}	Battery cycle life.
M	Large positive constant.
P^{BES}	Battery rated power.
P^{sch}	Scheduled wind power.
P^W	Actual wind power.
r	Interest rate.
RV	Battery residual value.
$\overline{SOC}, \underline{SOC}$	Maximum/Minimum state of charge.
T	Battery temperature.
Δh	Time interval duration.
δ^N	Number of time intervals.
ε	Convergence criterion.
η	Battery efficiency.
θ^{bat}	Battery degradation cost ($/Wh).

The associate editor coordinating the review of this manuscript and approving it for publication was Lei Wang.

ρ^{RT}	Real-time electricity market price.
ρ^{DA}	Day-ahead electricity market price.
σ	Battery self-discharge rate.
$\overline{\varphi}, \underline{\varphi}$	Maximum/Minimum range of the segment n.

C. BINARY VARIABLES

I	Discharge indicators.
U, D	Auxiliary binary variables.
w	Indicator of the selected value of the DOD.

D. VARIABLES

AG	Amount of the battery capacity fading.
C^{Deg}	Battery degradation cost ($).
DOD	Depth of discharge.
E^{BES}	Battery energy rating.
L^{BES}	Battery lifetime.
OF	Objective function.
P^{cu}	Curtailed power.
P^{ch}, P^{dch}	Charging/Discharging power.
P^{RT}	Power exchanged with the utility grid.
SOC	Battery state of charge.
SOH	Battery state of health.

I. INTRODUCTION

The intermittent nature of wind has a significant effect on the profits of wind farms and weakens their competitiveness in the electricity market [1]. In this regard, various solutions have been proposed to solve this challenge and improve the profitability of wind farms [2]. Among them, integrating batteries with wind farms has drawn more attention [3]. Recently, different battery types have been utilized next to the wind farms, among which lithium-ion batteries (LIBs) have received more attention due to their low self-discharge rate, high energy density, and lack of memory effect [4]. So that the LIBs currently compose more than 80% of the batteries installed internationally [5]. Nevertheless, diverse stress factors can degrade the LIB capacity and reduce its lifetime. Therefore, employing a suitable approach to maximize wind farm profits through batteries is one of the most considerable challenges for researchers [6].

Extensive studies have been conducted to achieve the optimal performance of the batteries in wind farms. A novel model predictive control (MPC)-based strategy for wind farms integrated with dual-battery is presented in [7] to improve the battery lifetime and the wind farm profit. A new stochastic programming based on Benders decomposition is proposed in [8] to calculate the optimal size of the battery under wind uncertainties. A stochastic bi-level optimization model for integrated wind-battery systems is provided in [9] to improve battery profits in energy and frequency regulation markets. A novel operation-planning model is presented in [10] to increase the participation of wind-battery systems in both the gas market and the day-ahead electricity market. A real-time approach for integrated wind-battery systems is provided in [11] to increase wind farm revenue; however, the battery degradation process (BDP) and its impact on the battery lifetime are ignored. It is worth noting that the BDP is one of the significant factors affecting the battery degradation cost (BDC) and the battery performance [12]. Due to the high investment costs of the LIB, it is necessary to integrate the BDC into the energy management problem to improve the financial analysis accuracy and increase the profitability of the LIB. In [13], [14], and [15], approximate models are proposed to incorporate the BDC in the LIB scheduling problem. In these models, the BDC is calculated in proportion to the amount of charging/discharging power. Nevertheless, the BDC should be calculated based on the BDP. As the BDC depends on different parameters, such as the LIB capital cost and the BDP, these methods can not accurately model the BDC.

There are two major approaches for modeling the BDP [16]. The first one is the data-driven approach, which estimates the battery state of health according to the laboratory data. In this regard, various machine learning techniques, such as neural networks, support vector machines, and gaussian process regression, are utilized to estimate the amount of the battery capacity fading [17]. Therefore, it is not required to mathematically model complex electrochemical reactions within the battery [18]. Nevertheless, the accuracy of data-driven approaches is highly dependent on the quality of the measured data. Moreover, these approaches have a high computational burden and require a lot of storage space [19].

The other one is the model-based approach, which estimates the state of health of the battery based on an electrical equivalent circuit model of the battery. In the existing literature, various model-based methods are introduced to calculate the LIB capacity fading due to the BDP. The model-based degradation methods can be categorized into two classes based on the nature of their implementation: empirical and theoretical models [19]. Empirical models [20], [21], [22], [23] are more convenient for analyzing and modeling the BDP in the energy management problem. Moreover, empirical models introduce a less computational burden to the optimization problem. In these models, the BDP is modeled based on experimental tests and under certain operational conditions. Thus, a model designed for a specific use of the LIB may not be usable in other positions. Therefore, to model and analyze the BDP, it will be essential to perform tests in accordance with the technical specifications of the battery and operational conditions. Nevertheless, the empirical models may not be economically justified for the battery owners due to time-consuming and expensive degradation tests [24].

Theoretical models [25], [26], [27], [28] analyze the electrochemical reactions inside the LIB and the factors affecting the loss of lithium-ion inventory (LLI) and loss of active cathode/anode material (LAM). In the battery energy management problem, the exact conditions of the LIB cells are unavailable; therefore, the BDP in theoretical models is estimated according to the battery usage patterns. Consequently, these methods cannot model and analyze the exact BDP in the battery scheduling stage in comparison with

TABLE 1. Comparison taxonomy of the reviewed papers.

Ref	Linear Model	Battery Lifetime	Battery State of Health	Cycle Aging Cost	Calendar Aging Cost	Cycle Counting Method
[13]				✓		
[14]	✓			✓		
[15]	✓	Cycle life		✓		
[31]		Cycle life				RFC algorithm
[32]		Cycle life		✓		RFC algorithm
[33]		Cycle life		✓		RFC algorithm
[34]		Cycle life	✓	✓		RFC algorithm
[35]	✓	Cycle life		✓		
[36]	✓	Cycle life	✓	✓		
[37]	✓	Cycle life	✓	✓		
[38]	✓	Cycle life	✓			
[39]	✓	Cycle life	✓	✓		
[40]	✓	Cycle life	✓	✓		
This Paper	✓	**Cycle/Calendar life**	✓	✓	✓	**Proposed algorithm**

empirical models [28]. Furthermore, due to the modeling complexity, employing these methods to model the BDP has a high computational burden on the optimization problem. This paper proposes a novel linear BDP model based on the semi-empirical model presented in [29] to minimize the disadvantages of the theoretical and empirical models. Moreover, the proposed model can be readily utilized in various applications of LIBs.

The BDC is estimated based on the amount of the LIB capacity fading and the relevant economic factors. The amount of LIB capacity fading stems from the cycle aging and the calendar aging [30]. The LIB cycle aging depends on the number of the performed cycles and the LIB depth of discharge (DOD) at each cycle. The LIB cycles are generally classified into complete and incomplete cycles. In complete cycles, the LIB discharge process begins from the full capacity and completes at the n^{th} DOD. Afterward, starting the LIB charging process, the LIB state of charge (SOC) will rise again to full capacity during an increasing path. On the other hand, after the discharge process completes in the incomplete cycles of the LIB, the SOC will be less than 100% during the charging process [28]. In [31], [32], [33], and [34], the rain-flow counting (RFC) algorithm is employed to count the complete and incomplete cycles of the LIB. As the RFC algorithm is nonlinearly modeled, it increases the computation time of the optimization problem and may get stuck in a locally optimal solution. In the other linear models presented in [35], [36], [37], [38], and [39], no distinction is made between the complete and incomplete cycles of the LIB. Moreover, the calendar aging process of the LIB is ignored in calculating the BDC. Therefore, these models are not able to efficiently calculate the BDC. In [40], a comprehensive home energy management system is presented to reduce the daily energy cost and the BDC; however, the effect of the calendar aging process on the battery state of health is neglected. Hence, the accuracy of the financial analysis and the proposed BDC model is decreased.

In conclusion, there are still numerous shortcomings in integrating the BDC into the LIB scheduling problem. To overcome the mentioned shortcomings, a linear comprehensive BDC model is presented in this paper. Table 1 shows a taxonomy to highlight the novelties of the proposed model in comparison with previous models. The main contributions of this paper can be summarized as follows.

- Providing a linear BDP model based on the semi-empirical approach aims to integrate the cycle aging and calendar aging of the LIB into the battery scheduling problem.
- Introducing a novel linear cycle counting algorithm to count complete/incomplete cycles and calculate the LIB cycle aging.
- Modeling the BDC and estimating the battery lifetime according to the cycle and calendar aging of the LIB.
- Presenting a novel MPC-based framework for optimal LIB energy management to reduce the battery capacity fading and the BDC.
- Investigating the impact of ignoring the LIB calendar aging process on the accuracy of the financial analyses and the obtained results.

The rest of the paper is organized as follows. In Section II, the BDP due to the cycle aging and calendar aging is linearly formulated, and then a novel approach is presented to calculate the BDC. In Section III, the energy management problem incorporating the BDP is formulated, then an MPC-based strategy is proposed to reduce the BDC and handle the uncertainty in the energy management problem. Section IV presents case studies that validate the applicability and performance of the proposed BDC model. Ultimately, concluding remarks are provided in Section V.

II. MODEL OUTLINE

The BDC stems from the loss of active cathode/anode material and the loss of lithium-ion inventory of the LIB [41]. Thus, to model the BDC in the LIB energy management problem, it is first necessary to model the factors affecting the BDP. Then the BDC can be calculated based on the amount of the LIB capacity fading and the pertinent economic parameters. All the contributing factors to the BDP are

linearly modeled in this section. Eventually, a novel procedure for estimating the BDC is presented.

A. LIB DEGRADATION MODEL

To consider the BDC in optimal LIB energy management problems, first and foremost, it is necessary to use an appropriate method to model the BDP and estimate its lifetime based on the charging/discharging pattern. Then, the BDC can be calculated at each time interval according to the amount of the LIB capacity fading.

As mentioned earlier, the BDP depends on the cycle and calendar aging process of the LIB. Cycle aging process stems from a decrease in the LIB lifetime per charging/discharging cycle due to the reduction in active lithium ions, and its amount depends on the battery temperature and the DOD in the charging/discharging process [29]. Calendar aging process is caused by the inherent degradation of the LIB during its lifetime, and it depends on the LIB temperature, SOC, and duration of LIB operation (from the time that the LIB has been manufactured in the factory to the current operational status). Therefore, if the LIB is not utilized, the state of health and capacity of the LIB will decrease due to the calendar aging process [38]. In this section, the cycle aging and calendar aging of the LIB are modeled to calculate the amount of the LIB capacity fading and the BDC. It should be noted that the limitations and assumptions of the proposed degradation model are as follows:

- The proposed cycle aging algorithm can calculate the cycle aging amount of all types of batteries. To this end, the relationship between the cycle life and the DOD of the battery is required. Furthermore, the amount of the battery SOC is needed at each time interval.
- The presented calendar aging model can be utilized to estimate the state of health of the LIBs. To model the calendar aging process of other types of batteries, it is necessary to do specific empirical tests and model their calendar aging process.
- As the air conditioning system is used for the installed LIB, the average temperature of the LIB is almost constant, and the range of temperature changes is small. Hence, a constant temperature can be considered for modeling the BDP [42].

1) BATTERY CYCLE AGING

As discussed, temperature changes in the battery are small; therefore, the LIB temperature can be considered steady [42]. Accordingly, it can be supposed that the LIB cycle aging is a function of the number of performed cycles and the DOD at each cycle.

The LIB cycles are categorized into two groups: the complete and incomplete cycles. A nonlinear method based on the RFC algorithm is presented in [32] to count the number of the complete and incomplete cycles of the LIB. As using nonlinear constraints in the optimization problem increases the computation time, a novel linear algorithm is proposed in this paper to calculate the LIB cycle aging according to the DOD at each complete/incomplete cycle. Fig. 1 displays the flowchart of the proposed algorithm for calculating the LIB cycle aging. In the first step, the SOC profile is analyzed to find the local maximum and minimum values of the SOC profile following a continuously declining path. This process is repeated until all peaks (beginning of the LIB discharging process) and valleys (end of the LIB discharge process) of the SOC profile are determined. In the proposed algorithm, equations (1)-(2) are utilized to determine the peaks and valleys of the SOC profile.

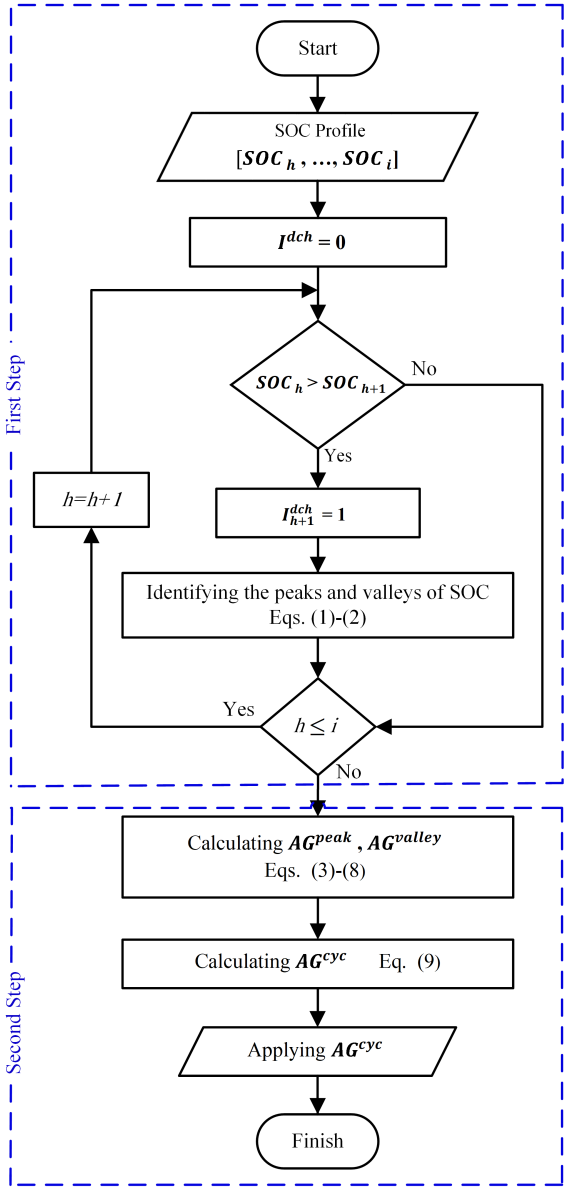

FIGURE 1. Cycle aging estimation algorithm.

$$U_h^{dch} - D_h^{dch} = I_{(h+1)}^{dch} - I_h^{dch} \quad \forall h \in \Omega^h \tag{1}$$

$$U_h^{dch} + D_h^{dch} \leq 1 \quad \forall h \in \Omega^h \tag{2}$$

where the binary variable I_h^{dch} indicates the battery discharge status, and during the discharge process, its value will be

equal to 1, otherwise 0. According to formulas (1) and (2), when the battery discharge process starts, the value of the binary variable U_h^{dch} will be equal to 1, otherwise 0. Similarly, when the battery discharge process is complete, the binary variable D_h^{dch} will be 1, otherwise 0. In other words, the binary variables U_h^{dch} and D_h^{dch} will be equal to 1 at the local maximum and minimum values of the SOC profile, respectively.

In the second step, the LIB cycle aging is calculated based on the complete and incomplete cycles. The incomplete cycles can be estimated by the superposition principle and converting an incomplete cycle into two complete cycles. For example, according to Fig. 2, the incomplete-cycle IC1 can be considered equivalent to subtracting the complete-cycle C2 from the complete-cycle C1. Assuming the C2-DOD is equal to the IC-start DOD, and the C2-DOD is equal to the IC1-end DOD. Equations (3)-(4) are employed to calculate the LIB cycle aging due to the complete and incomplete cycles. Equation (3) shows the LIB cycle aging at the local minimum SOC (valley). Similarly, the LIB cycle aging at the local maximum SOC (peak) is calculated by equation (4).

$$AG_h^{peak} = AG_h U_h^{dch} \quad \forall h \in \Omega^h \tag{3}$$

$$AG_h^{valley} = AG_h D_h^{dch} \quad \forall h \in \Omega^h \tag{4}$$

where AG indicates the amount of the LIB capacity fading which is calculated by equation (5). In this equation, E^{ins} shows the LIB initial capacity, subscript n denotes the DOD value index, N^{fail} indicates the battery cycle life, and w_{hn} is a binary variable that shows the value of DOD for the discharge segment n. The value of w_{hn} is determined by equations (6)-(8).

$$AG_h = \begin{cases} \sum_n \dfrac{0.2E^{ins}}{N_n^{fail}} w_{hn} & n \neq 0 \\ 0 & Otherwise \end{cases} \quad \forall h \in \Omega^h \tag{5}$$

$$DOD_h = E_h^{BES} - SOC_h \quad \forall h \in \Omega^h \tag{6}$$

$$\sum_n \underline{\varphi_n} E_h^{BES} w_{hn} \leq DOD_h \leq \sum_n \overline{\varphi_n} E_h^{BES} w_{hn} \quad \forall h \in \Omega^h \tag{7}$$

$$\sum_n w_{hn} \leq 1 \quad \forall h \in \Omega^h \tag{8}$$

where $\overline{\varphi}$ and $\underline{\varphi}$ are the maximum and minimum DOD for segment n, DOD is the battery depth of discharge, and SOC is the state of charge. Equation (6) shows the amount of the battery DOD. According to equations (7)-(8), when the DOD is between $\underline{\varphi_n} E_h^{BES}$ and $\overline{\varphi_n} E_h^{BES}$, the binary variable w_{hn} for the DOD n will be equal to 1; otherwise 0. In other words, w_{hn} represents the chosen DOD segment. Eventually, the amount of the LIB cycle aging is calculated by equation (9).

$$AG_h^{cyc} = AG_h^{valley} - AG_h^{peak} \quad \forall h \in \Omega^h \tag{9}$$

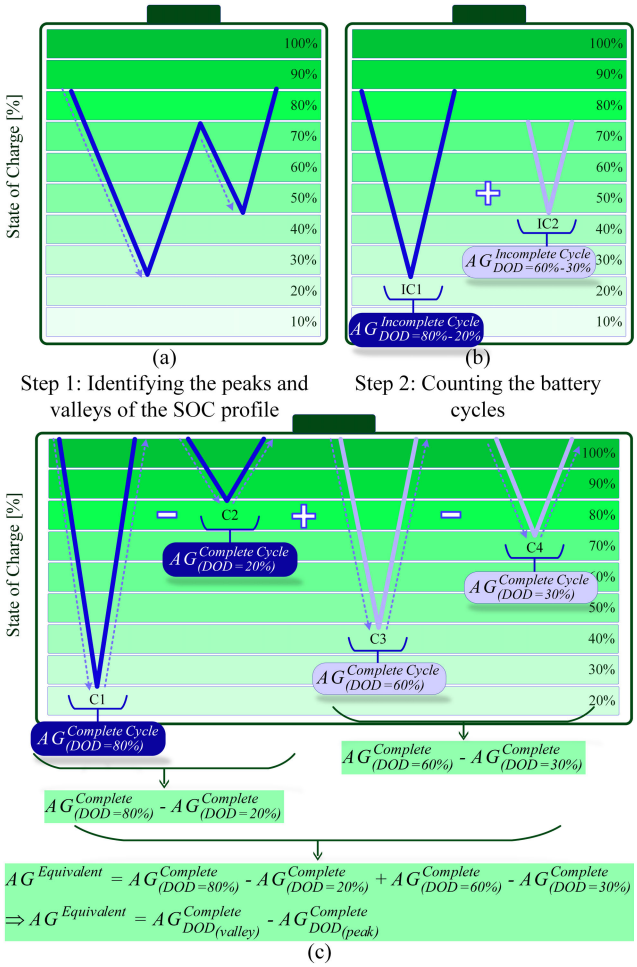

FIGURE 2. Battery cycle aging calculation approach.

It is worth noting that the non-linear term of constraint (3), the multiplication of binary variable U^{dch} and the continuous variable AG can be linearized using a new bilinear variable LAG and constraints (10) and (11) as follows:

$$0 \leq LAG_h \leq MU_h^{dch} \quad \forall h \in \Omega^h \tag{10}$$

$$AG_h - M\left(1 - U_h^{dch}\right) \leq LAG_h \leq AG_h + M\left(1 - U_h^{dch}\right) \quad \forall h \in \Omega^h \tag{11}$$

where M is a large positive constant. According to (10), if U^{dch} is 0, LAG would be 0. On the other hand, if U^{dch} is 1, constraint (10) is relaxed, and according to (11), LAG would be equal to AG. Hence, the non-linear term of constraint (3) is linearized by constraints (10) and (11). Similarly, the non-linear term of equations (4) and (7), the multiplication of the binary variable and continuous variable, are linearized using constraints (10) and (11).

2) BATTERY CALENDAR AGING

According to the semi-empirical model presented in [29], the LIB calendar aging (AG^{cal}) can be calculated by nonlinear

equation (12). In this equation, h shows the installation time (hour), SOC is the state of charge (%), and T is the LIB temperature (°C).

$$AG_h^{cal} = \left(\frac{h}{720}\right)^{0.8}(0.019SOC_h^{0.823} + 0.5195) \times(3.258 \times 10^{-9}T_h^{5.087} + 0.295) \quad \forall h \in \Omega^h \quad (12)$$

Assuming the LIB temperature is constant, the LIB cycle aging is a function of time and SOC. Hence, the LIB calendar aging can be modeled by equation (13).

$$AG_h^{cal} = \left(\frac{h}{720}\right)^{0.8}(0.0064SOC_h^{0.823} + 0.1751) \quad \forall h \in \Omega^h \quad (13)$$

The equation (13) is linearized by regression method, and then the LIB calendar aging can be modeled with the help of linear relation (14). The LIB calendar aging is calculated according to the LIB capacity (E^{BES}) and the SOC using equation (15). Finally, equation (16) models the amount of the LIB capacity fading due to the calendar aging process at time interval h.

$$AG_h^{cal} = \left(\frac{h}{720}\right)^{0.8}(0.0028SOC_h + 0.1939) \quad \forall h \in \Omega^h \quad (14)$$

$$AG_h^{cal} = \left(\frac{h}{720}\right)^{0.8}(0.0028SOC_h + 0.001939E_h^{BES}) \quad \forall h \in \Omega^h \quad (15)$$

$$AG_h^{cal} = \left[\left(\frac{h}{720}\right)^{0.8} - \left(\frac{h-1}{720}\right)^{0.8}\right](0.0028SOC_h + 0.001939E_h^{BES}) \quad \forall h \in \Omega^h \quad (16)$$

B. BATTERY DEGRADATION COST

The BDC refers to the battery depreciation cost and depends on the degradation process, the lifetime, and the investment cost of the battery. Fig. 3 demonstrates the concept of the BDC. As shown, the total BDC during the battery lifetime is equal to the difference between the purchase price and the residual (salvage) value of the battery. Due to the high investment cost and the limited lifetime of batteries, it is necessary to integrate the BDC into the battery scheduling problem. Ignoring the cost of battery degradation considerably reduces the accuracy of the financial analysis. In order to improve the accuracy of the obtained results, a comprehensive model for modeling the BDC is presented in this section.

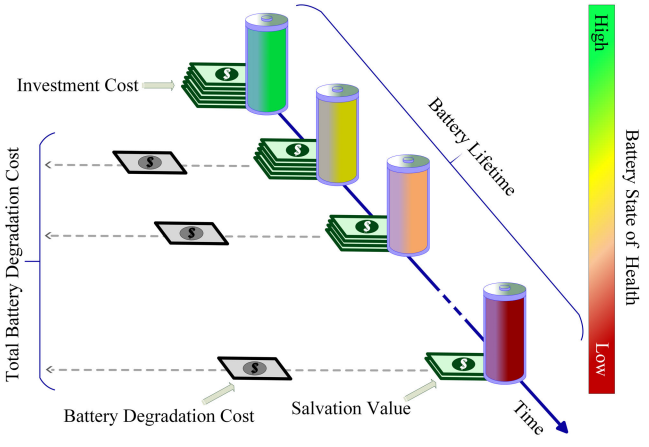

FIGURE 3. Schematic illustration of the battery degradation cost concept.

As discussed, the LIB lifetime depends on the calendar aging and the cycle aging of the battery. As the amount of the BDP is different at each time interval, a constant value cannot be used to model the BDC. Hence, this paper presents a novel method to estimate the BDC based on the BDP at each time interval. The proposed method is modeled by equations (17)-(20).

$$L_h^{BES} = \frac{0.2E^{ins}}{AG_h} \quad \forall h \in \Omega^h \quad (17)$$

$$C_h^{Deg} = \frac{r\left(IC(1+r)^{\frac{0.2E^{ins}}{AG_h}} - RV\right)}{(1+r)^{\frac{0.2E^{ins}}{AG_h}} - 1} \quad \forall h \in \Omega^h \quad (18)$$

$$IC = E^{ins}(C^E + C^n) + P^{BES}C^P \quad (19)$$

$$\theta_h^{bat} = \frac{C_h^{Deg}}{AG_h} \quad \forall h \in \Omega^h \quad (20)$$

where L^{BES} is the LIB lifetime, C^{Deg} is the BDC, r is the interest rate, RV is the LIB residual value, C^E is the LIB energy rating cost, C^n is the LIB installation cost, P^{BES} is the LIB power rating, and C^P is the power rating cost. When the LIB loses 20% of its initial capacity, its lifetime ends [38]. Hence, the battery lifetime can be estimated according to the amount of the LIB capacity fading using equation (17). By calculating the LIB lifetime, the LIB degradation cost (C^{Deg}) is modeled by equation (18) as a series of equal payments over the LIB lifetime. In this equation, IC denotes the LIB capital cost and it is determined by equation (19). The BDC associated with 1 Wh of the LIB capacity fading (θ^{bat}) is determined by equation (20).

The main contributing factors to the BDP were linearly modeled in this section. Then a novel BDC model was presented. In the remainder of the paper, the proposed BDC model will be integrated into the battery energy management problem to investigate its applicability and effectiveness.

III. PROBLEM FORMULATION

The main factors affecting the BDP were linearly modeled in the previous section. Also, a novel BDC model was presented to estimate the BDC based on the amount of the LIB lifetime and the relevant financial parameters. In this section, the BDC is integrated into the LIB scheduling problem, and the associated scheduling problem is formulated as a Mixed Integer Linear Programming (MILP) model. Then, a novel predictive energy management strategy (PEMS) is proposed

to solve the optimization problem and address the uncertainty in the energy management problem.

A. OBJECTIVE FUNCTION AND CONSTRAINTS

In the proposed framework, the scheduling problem is formulated to maximize the wind farm profit by selling committed power and reducing the BDC. In this regard, the objective function and operation constraints of the scheduling problem over the time intervals $\Omega^h = [t+1,\ldots, t+k]$ are defined as follows:

$$OF = \sum_{h=t+1}^{t+k} \left(\rho_h^{DA} P_h^{sch} - \rho_h^{RT} P_h^{RT} - C_h^{cyc} - C_h^{cal}\right) \quad (21)$$

$$C_h^{cyc} = \theta_h^{bat} AG_h^{valley} - \theta_h^{bat} AG_h^{peak} \quad \forall h \in \Omega^h \quad (22)$$

$$C_h^{cal} = \theta_h^{bat} AG_h^{cal} \quad \forall h \in \Omega^h \quad (23)$$

$$P_h^{sch} = P_h^W + P_h^{ch} + P_h^{dch} + P_h^{RT} + P_h^{cu} \quad \forall h \in \Omega^h \quad (24)$$

$$-P_h^W \le P_h^{cu} \le 0 \quad \forall h \in \Omega^h \quad (25)$$

$$P_h^{RT} \ge 0 \quad \forall h \in \Omega^h \quad (26)$$

where OF is the objective function, P^{sch} is the scheduled wind power, ρ^{DA} is the day-ahead market price, P^{RT} is the purchased power from the real-time market, ρ^{RT} is the real-time market price, P^W is the actual wind generation power, P^{cu} is the curtailed wind power, and P^{ch}/P^{dch} are the LIB charging/discharging power. The objective function (21) shows the amount of wind farm income and expenses during the scheduling horizon. The first term of the objective function represents the wind farm income from the sale of committed power. The second term of this relationship shows the cost of purchasing energy from the real-time electricity market to compensate for the forecast error. The third term of the objective function reveals the cycle aging cost (C^{cyc}), which is modeled by equation (22) in the optimization problem. The last term of the objective function (21) models the calendar aging cost (C^{cal}) during the scheduling horizon. The calendar aging cost is estimated by equation (23). The power balance equation (24) shows the parity of the committed generation power with the power supplied by the wind farm. Accordingly, when the actual wind power is greater than the committed power, the excess power is stored by the LIB or curtailed. Similarly, when the actual wind power is less than the committed power, the real-time market and the LIB provide a lack of power. Constraint (25) shows the curtailed wind power [13]. Constraint (26) demonstrates the amount of power purchased from the real-time market. Other LIB operation constraints are modeled by (27)-(32).

$$0 \le P_h^{dch} \le P^{BES} I_h^{dch} \quad \forall h \in \Omega^h \quad (27)$$

$$-P^{BES}(1 - I_h^{dch}) \le P_h^{ch} \le 0 \quad \forall h \in \Omega^h \quad (28)$$

$$SOC_h = SOC_{(h-1)}(1-\sigma) - \frac{P_h^{dch}\Delta h}{\eta^{dch}} - \eta^{ch} P_h^{ch} \Delta h \quad \forall h \in \Omega^h \quad (29)$$

$$E_h^{BES}\underline{SOC} \le SOC_h \le E_h^{BES}\overline{SOC} \quad \forall h \in \Omega^h \quad (30)$$

$$E_h^{BES} = E_{(h-1)}^{BES} - AG_h^{cyc} - AG_h^{cal} \quad \forall h \in \Omega^h \quad (31)$$

$$SOH_h = \frac{E_h^{BES}}{E^{ins}} \quad \forall h \in \Omega^h \quad (32)$$

where σ is the LIB self-discharge rate, Δh is the time interval duration, SOH is the LIB state of health, and $\overline{SOC}/\underline{SOC}$ are the maximum and minimum state of charge, respectively. Limitations of the discharging and charging power of the LIB are modeled by constraints (27) and (28), respectively. The binary variable I_h^{dch} shows the LIB discharge status and will be equal to 1 during the discharge process. The stored energy in the LIB at time interval h is equal to the stored energy in the previous time interval (h-1) minus the charged or discharged energy at time interval h (29). In (30), the SOC is restricted by the LIB capacity at each time interval. Due to the BDP during the scheduling horizon, the available LIB capacity at each time interval can be calculated by the state equation (31). The second term of equation (31) indicates the amount of LIB capacity fading due to the cycle aging process and is calculated using equations (1)-(11). The third term of equation (31) demonstrates the amount of the LIB capacity fading due to the calendar aging process and is calculated by equation (16). Finally, the LIB state of health is determined by equation (32).

B. PREDICTIVE ENERGY MANAGEMENT STRATEGY

Real-time market price and wind output power can considerably affect the wind farm profit and the LIB performance. In the presented framework, a novel PEMS according to the MPC is provided to handle the uncertainty in the input parameters (real-time market price and wind power generation) and improve the LIB performance. The principal advantage of the MPC is that it can indirectly address the uncertainty in the scheduling problem [43]. In the MPC controller, the system behavior is anticipated for a fixed time horizon, known as the prediction horizon, and the scheduling problem is solved over the prediction horizon [44]. Then, the first control signal is applied. As the optimization and prediction processes are repeated at each time interval, the system can take more appropriate operational measures in response to unexpected changes [45].

The proposed PEMS framework for solving the LIB scheduling problem is demonstrated in Fig. 4. In the first step, the required data (including the meteorological information, the historical price of the real-time market, the LIB specifications, and the committed wind power) is collected. In time interval t, the real-time market price and wind power generation are forecasted from $t+1$ to $t+k$. An initial value for θ^{bat} is also considered. In the next step, the LIB energy management problem is solved over the prediction horizon. The associated energy management problem is modeled by equations (1)-(11), (16), and (21)-(32). Afterward,

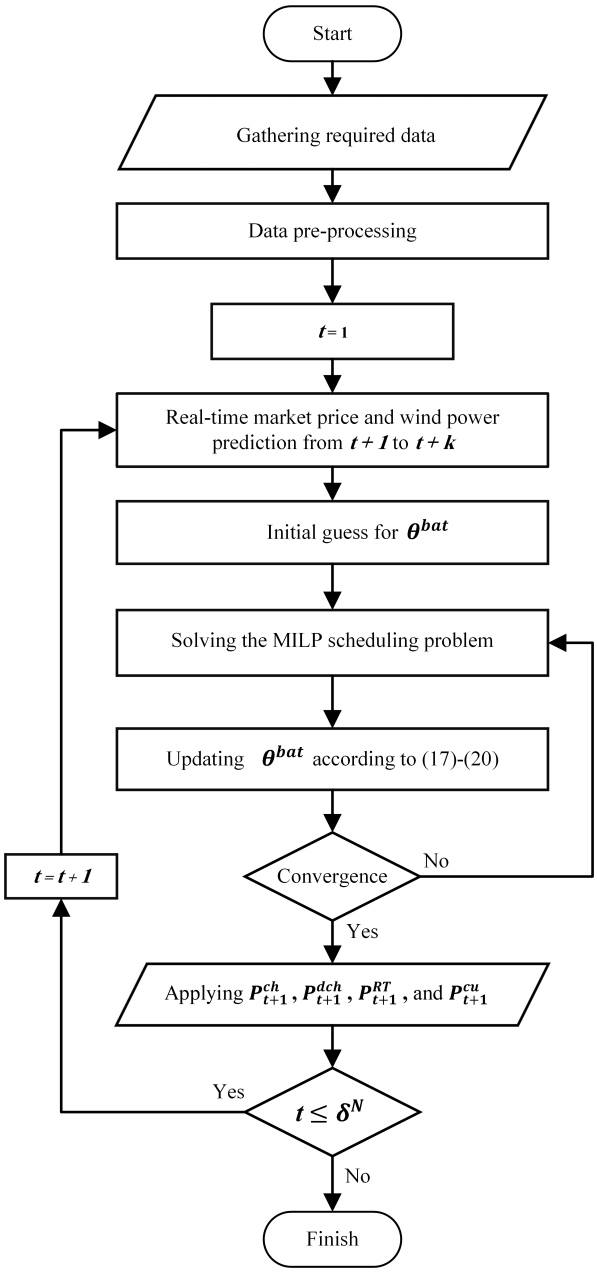

FIGURE 4. Proposed framework for integrating the BDC into the LIB scheduling problem.

the new value of θ^{bat} is calculated by equations (17)-(20). In the next step, $\theta^{bat,new}$ is compared to its previous value $\theta^{bat,old}$. If the first terminating constraint (33) is activated, the system processes the first control signal and goes to the next time interval. Otherwise, using the θ^{bat} obtained from the latest iteration, the optimization problem is solved again. The proposed iterative method should be followed until the second terminating constraint is met. In equation (33), the ε indicates the convergence criterion and is set to 2% in the numerical simulations of the paper. It should be noted that the value of the ε can be chosen less to improve the accuracy of the obtained results, in which case the number of simulation iterations and the simulation time will increase. In case of practical use of the proposed framework, the value of ε can be reduced to more accurately model the BDC in the battery scheduling problem.

$$\frac{\left|\theta_h^{bat,old} - \theta_h^{bat,new}\right|}{\theta_h^{bat,old}} \leq \varepsilon \quad \forall h \in \Omega^h \tag{33}$$

IV. SIMULATION RESULTS

A. CASE STUDY

To evaluate the effectiveness of the proposed BDC model, three LIBs (B1, B2, and B3) with various initial capacity is applied. The characteristics of the LIBs are indicated in Table 2. In the proposed PEMS, an artificial neural network is used to predict the wind farm generation power and the real-time electricity market price. The required data for prediction are collected from the Sotavento wind farm [46]. The associated scheduling problem is formulated as a MILP model, which is solved by CPLEX 12.8 and runs on an Intel Core i7-4500U 2.4 GHz personal computer with 6 GB of RAM.

TABLE 2. Battery characteristics.

Battery	E^{ins} (kWh)	P^{BES} (kW)	C^E ($/kWh)	C^P ($/Wh)	C^n ($/kWh)
B1	800	600	290	230	20
B2	600	400	290	230	20
B3	400	300	290	230	20

Five cases pertaining to the LIB optimal scheduling are defined to evaluate the abilities of the proposed approach as below:

Case 1: The BDP is ignored in the scheduling problem.

Case 2: The cycle aging process is considered to improve the LIB performance, but the LIB calendar aging is neglected.

Case 3: The calendar aging process is integrated into the LIB scheduling problem, but the LIB cycle aging process is ignored.

Case 4: The cycle aging and calendar aging are considered to improve the accuracy of the obtained results.

Case 5: The RFC algorithm is employed to evaluate the modeling accuracy of the proposed cycle counting algorithm.

B. NUMERICAL RESULTS

Case 1: In this case, the proposed PEMS framework is employed to address the uncertainty in the input parameters and improve the LIB performance; however, the BDP is ignored. In the proposed strategy, the wind farm generation power and the real-time market price are predicted at each time interval for a fixed time horizon. Then, these values are used for determining the LIB charging/discharging strategy. Fig. 5 and Fig. 6 indicate the wind power generation and the power profile, respectively. As illustrated, when the production power of the wind farm is less than the committed power, the power shortage is compensated by the LIB or the purchase from the real-time market. Otherwise, when the wind generation power is more than the committed power, the extra power is stored by the LIB or curtailed. As shown

TABLE 3. Numerical simulation results for batteries under study.

Case	Cycle Aging (Wh)			Cycle Aging Cost ($)			Calendar Aging (Wh)			Calendar Aging Cost ($)			Wind Farm Profit ($)		
	B1	B2	B3	B1	B2	B3	B1	B2	B3	B1	B2	B3	B1	B2	B3
Case 1	–	–	–	–	–	–	–	–	–	–	–	–	12399.26	12370.64	12335.90
Case 2	32	27	21	37.38	26.88	21.24	–	–	–	–	–	–	12346.93	12332.79	12309.58
Case 3	–	–	–	–	–	–	152	113	74	206.37	132.11	89.75	12182.47	12233.15	12241.56
Case 4	26	24	16	28.96	22.89	15.91	144	108	71	197.41	127.03	86.10	12141.53	12202.89	12220.34

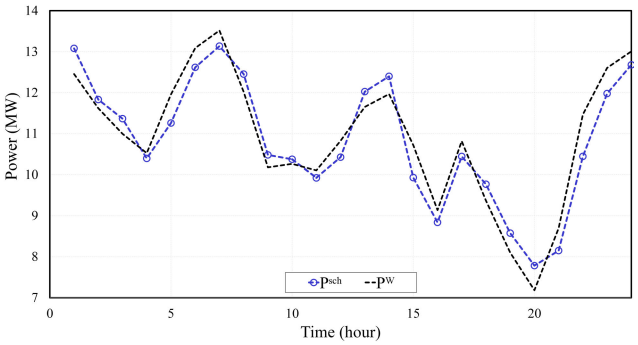

FIGURE 5. Committed and actual wind power.

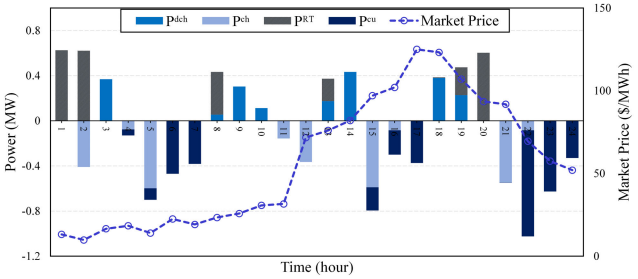

FIGURE 6. ILB charging/discharging power profile and purchasing power in Case 1-B1.

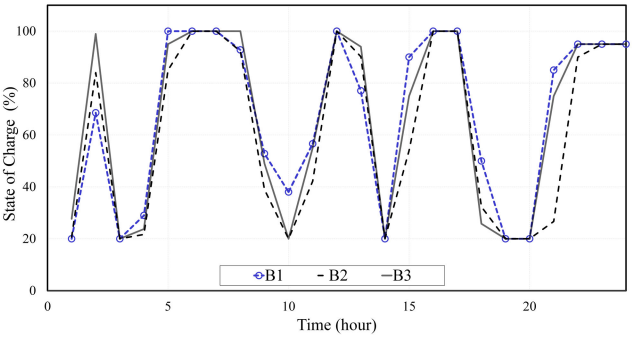

FIGURE 7. Optimal charging/discharging strategies for Case 1.

in Table 3 and Fig. 7, the battery-B1 contributes the most to compensate for the prediction error; hence it obtains the most profit for the wind farm. However, the obtained results are not accurate because of ignoring the BDP. In the rest of this section, the BDP is integrated into the optimization problem to improve the accuracy of financial analyzes.

Case 2: In this case, the proposed cycle counting algorithm in Section II is utilized to calculate the LIB cycle aging. Furthermore, the presented procedure in Section III is used to integrate the cycle aging cost into the LIB scheduling problem. As seen in Table 3, the battery-B1 creates more profit for the wind farm than other LIBs. However, due to considering the cycle aging process in the optimization problem, the wind farm profit is reduced by 0.42% compared to Case 1. It should be noted that the BDP is due to the electrochemical reactions inside the LIB, which reduce the lifetime and the capacity of the LIB. For this reason, the impact of the BDP on the performance and lifetime of the LIB should be considered. Fig. 8 and Fig. 9 illustrate the optimal SOC and the cycle aging cost of the LIBs, respectively. As shown, the cycle aging cost is calculated according to the DOD at each cycle, and it depends on the amount of capacity fading and the capital cost of the LIB. As mentioned in Section II, the proposed algorithm for calculating cycle aging of incomplete cycles uses the superposition principle and converts an incomplete cycle into two complete cycles; consequently, the BDC is estimated for each incomplete cycle based on the superposition principle. The sensitivity of the battery cycle aging cost to the temperature and DOD is indicated in Fig. 10. As shown, the BDC increases as the temperature and DOD of the battery increase. Thus, if the effect of the DOD on the cycle aging process of the battery is neglected, the accuracy of the obtained results will be decreased. Furthermore, this figure shows that the sensitivity of the battery cycle aging cost to the DOD at the high DODs is much more than at the low DODs. Therefore, the performance of the proposed model at the high DODs is considerably influenced by the accuracy of DOD estimation.

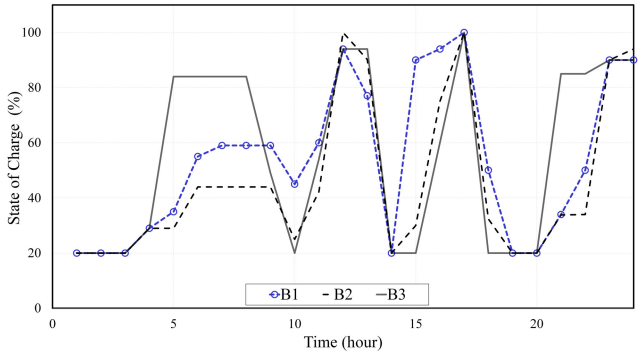

FIGURE 8. Optimal charging/discharging strategies of Case 2.

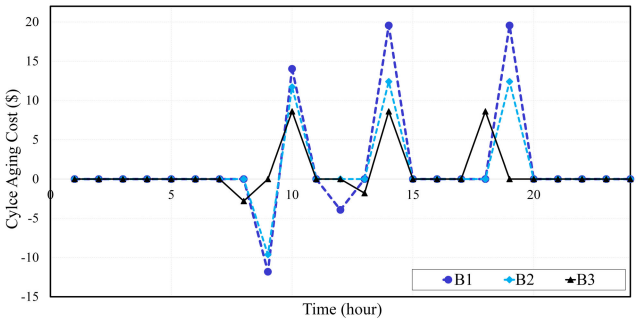

FIGURE 9. LIB cycle aging cost for the proposed strategies of Case 2.

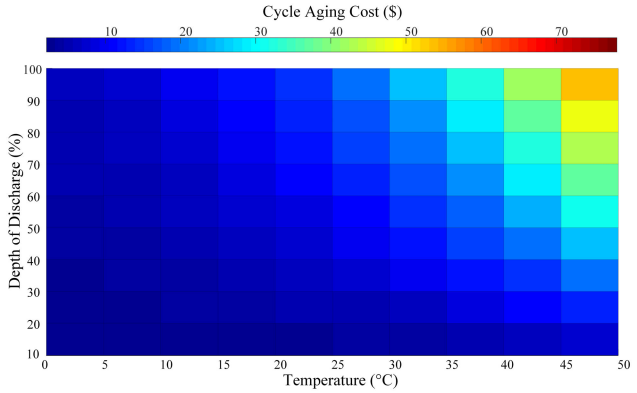

FIGURE 10. Sensitivity of the battery cycle aging cost to the depth of discharge and temperature of the battery-B1.

Case 3: In this case, the LIB calendar aging is integrated into the LIB energy management problem to improve the accuracy of the financial analysis. To this end, equation (16) is employed to model the calendar aging process in the optimization problem. However, the LIB cycle aging process is ignored. Fig. 11 and Fig. 12 show the optimal charging/discharging strategies and calendar aging cost of the batteries, respectively. As demonstrated, the LIB calendar aging cost is distinct for each SOC. Thus, to use the LIB more efficiently and reduce the calendar aging cost, the effect of the SOC on the calendar aging process should be considered in the battery scheduling problem. Furthermore, Fig. 12 shows that the amount of calendar aging at each time interval declines as time passage. Thus, the LIB calendar aging cost would be much lower in the last years of the LIB lifetime than in the first years. Therefore, the passage of time should be considered in modeling the calendar aging cost to improve the accuracy of financial analysis and more efficient LIB use. As the calendar aging cost is integrated into the optimization problem, the B1 no longer provides the maximum benefit to the wind farm. As shown in Table 3, the profit of the wind farm will be increased by 0.49% if the battery-B3 is employed. These results indicate that a larger battery does not necessarily provide more economic benefits for the wind farm.

Case 4: In this case, the cycle aging and calendar aging of the LIB are integrated into the battery scheduling problem. As shown in Fig.13, due to the integration of the cycle aging and calendar aging processes in the LIB scheduling problem, the contribution of the LIB in compensating for the prediction error is reduced. Hence, according to Table 3, the wind farm profit has decreased compared to the other case studies. Nevertheless, in case the calendar aging and cycle aging processes are determined for the proposed strategies by other case studies, the actual wind farm profit would differ from the obtained results in Table 3. To evaluate the effect of neglecting the BDP on the accuracy of the financial analysis, the numerical simulation is done to calculate the BDC of the proposed strategies by other case studies. Fig. 14 and Fig. 15 show the amount of the BDC and the actual profit of the wind farm according to the proposed charging/discharging strategies, respectively. As shown, the proposed charging/discharging strategy by Case 4 imposes the lowest BDC. Moreover, this strategy would create the most wind farm profit compared to other charging/discharging strategies. These results demonstrate that neglecting the BDP significantly declines the accuracy of financial analyses. Also, comparing the results of Case 4 reveals that battery-B3 provided more profit for the wind farm. This result highlights the importance of considering the cycle aging and calendar aging processes in determining the optimal battery capacity.

Case 5: In this case, the accuracy of the presented cycle counting algorithm is investigated. In the existing literature,

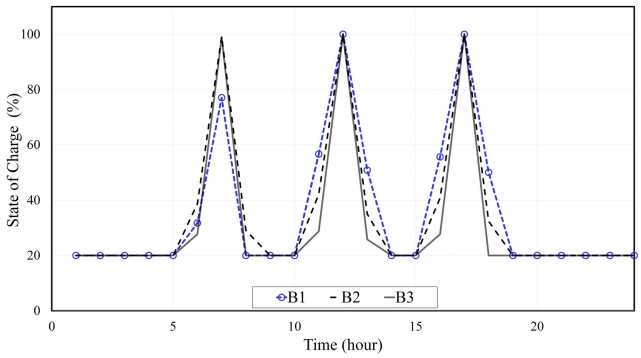

FIGURE 11. Optimal charging/discharging strategies of Case 3.

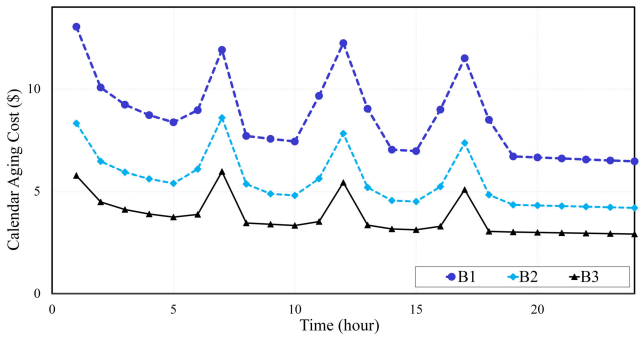

FIGURE 12. LIB calendar aging cost for the proposed strategies of Case 3.

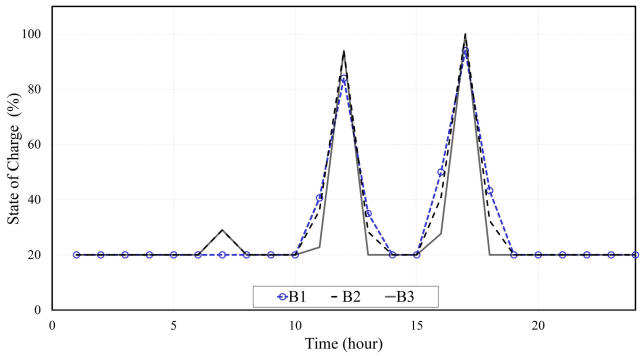

FIGURE 13. Optimal charging/discharging strategies of Case 4.

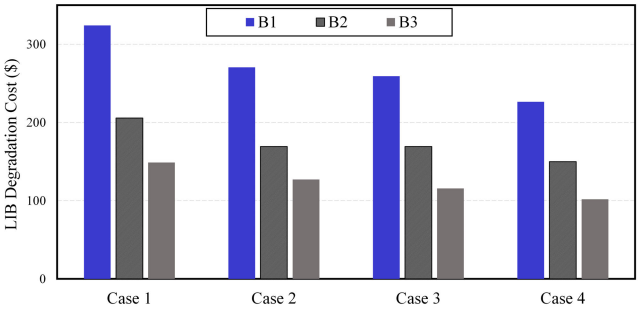

FIGURE 14. BDC of the proposed strategies.

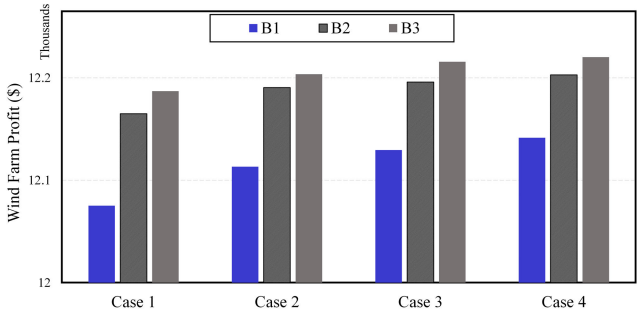

FIGURE 15. Actual profit of the wind farm for proposed strategies.

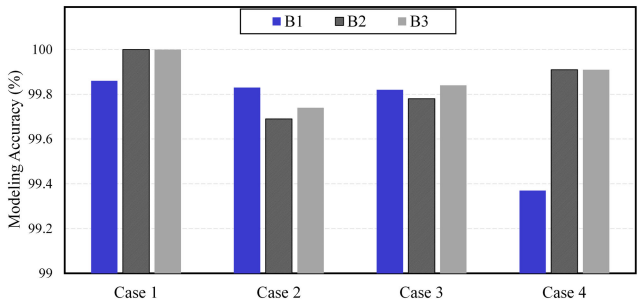

FIGURE 16. Comparing the performance of the proposed cycle counting algorithm with the RFC algorithm.

the RFC algorithm is employed to model the cycle aging process of the battery due to the complete and incomplete cycles. The effectiveness and applicability of this algorithm are verified in [31], [32], [33], and [34]. Therefore, the RFC algorithm is used to evaluate the accuracy and performance of the proposed algorithm. Accordingly, the amounts of the battery cycle aging due to the proposed charging/discharging strategies of the previous case studies are calculated by the RFC algorithm. Fig. 16 indicates the modeling accuracy of the proposed algorithm in comparison with the RFC algorithm. As demonstrated, the modeling accuracy of the proposed algorithm in the worst case is equal to 99.37%. Moreover, these results reveal that the presented algorithm can accurately estimate the amount of the battery cycle aging due to the complete and incomplete cycles. It is worth noting that the modeling accuracy of the proposed algorithm depends on the number of linearization segments, and the linearization error decreases as the number of segments increases.

V. CONCLUSION

In this paper, a novel mathematical formulation has been presented to integrate the BDC into the LIB energy management problem. The BDC has been modeled according to the pertinent financial factors and the amount of the cycle/calendar aging process of the LIB. In this regard, a linear cycle counting algorithm is introduced to calculate the LIB cycle aging. In this algorithm, firstly, the local maximum and minimum values of the SOC profile are identified by the proposed linear formulations. Then the superposition principle is used to convert incomplete cycles into complete cycles. In the BDC model, the main contributing factors to the calendar aging process of the LIB are also incorporated into the BDP model. Finally, a novel predictive energy management strategy is proposed to efficiently decrease the BDC and handle the uncertainty in the associated optimization problem. Various case studies have been investigated to evaluate the effectiveness and efficiency of the proposed BDC model. The key conclusions drawn from the study are summarized as follows.

- Considering the BDC in the LIB energy management problem significantly affects the optimal charging/discharging strategy and can play a critical role in increasing the profit of the LIB owners. Based on the simulation results, the actual wind farm profit has increased by 1.21%, compared to the case where the BDC has been neglected. Also, the BDC and the amount of capacity fading of the LIB have decreased by 30.16% and 32.81%, respectively.
- Ignoring the calendar aging process of the LIB in the energy management problem leads to non-optimized charging/discharging strategies. In case the LIB cycle and calendar aging have been integrated into the optimization problem, the amount of the LIB capacity fading and the BDC have declined by 22.94% and 16.36%, respectively, compared to when only the cycle aging process has been considered.
- As the amount of the LIB calendar aging is gradually reduced as time passage, ignoring the passage of time

in the BDC modeling decreases the accuracy of the economic analyses and obtained results.

The proposed battery degradation model can be implemented to calculate the amount of the battery capacity fading for various applications of the LIB. For future studies, it is suggested to determine the optimal size of the battery based on the cycle aging and the calendar aging processes in order to increase the profitability of the battery. Moreover, further research should be conducted on the optimal operating temperature of the battery based on the BDP and the investment cost of the air conditioning system.

REFERENCES

[1] G. Zhang, F. Li, and C. Xie, "Flexible robust risk-constrained unit commitment of power system incorporating large scale wind generation and energy storage," *IEEE Access*, vol. 8, pp. 209232–209241, 2020.

[2] S. Esmaeili, M. Amini, A. Khorsandi, S. H. Fathi, S. H. Hosseinian, and J. Millimonfared, "Market-oriented optimal control strategy for an integrated energy storage system and wind farm," in *Proc. 29th Iranian Conf. Electr. Eng. (ICEE)*, May 2021, pp. 407–411.

[3] M. K. Metwaly and J. Teh, "Optimum network ageing and battery sizing for improved wind penetration and reliability," *IEEE Access*, vol. 8, pp. 118603–118611, 2020.

[4] M. A. Hannan, M. M. Hoque, A. Hussain, Y. Yusof, and P. J. Ker, "State-of-the-art and energy management system of lithium-ion batteries in electric vehicle applications: Issues and recommendations," *IEEE Access*, vol. 6, pp. 19362–19378, 2018.

[5] K. Mongird, V. V. Viswanathan, P. J. Balducci, M. J. E. Alam, V. Fotedar, V. S. Koritarov, and B. Hadjerioua, "Energy storage technology and cost characterization report," Pacific Northwest Nat. Lab., Richland, WA, USA, Tech. Rep. PNNL-28866, 2019.

[6] W. Jung, J. Jeong, J. Kim, and D. Chang, "Optimization of hybrid off-grid system consisting of renewables and Li-ion batteries," *J. Power Sources*, vol. 451, Mar. 2020, Art. no. 227754.

[7] B. Wang, G. Cai, and D. Yang, "Dispatching of a wind farm incorporated with dual-battery energy storage system using model predictive control," *IEEE Access*, vol. 8, pp. 144442–144452, 2020.

[8] M. A. Abdulgalil, M. Khalid, and F. Alismail, "Optimizing a distributed wind-storage system under critical uncertainties using benders decomposition," *IEEE Access*, vol. 7, pp. 77951–77963, 2019.

[9] P. Li, Z. Wang, and J. Jin, "Market impact of wind-energy storage alliance strategic bidding under uncertainty," *IEEE Access*, vol. 9, pp. 156537–156547, 2021.

[10] R. A. Kordkheili, M. Pourakbari-Kasmaei, M. Lehtonen, R. A. Kordkheili, and E. Pouresmaeil, "Multi-alternative operation-planning problem of wind farms participating in gas and electricity markets," *IEEE Access*, vol. 9, pp. 166825–166837, 2021.

[11] Z. Guo, W. Wei, L. Chen, Y. Chen, and S. Mei, "Real-time self-dispatch of a remote wind-storage integrated power plant without predictions: Explicit policy and performance guarantee," *IEEE Open Access J. Power Energy*, vol. 8, pp. 484–496, 2021.

[12] M. Amini, S. Esmaeili, M. Sayadlou, A. Khorsandi, and S. H. Hosseinian, "A real time MPC-based strategy for PV plant with battery energy storage," in *Proc. 30th Int. Conf. Electr. Eng. (ICEE)*, May 2022, pp. 946–950.

[13] S. S. K. Madahi, A. S. Kamrani, and H. Nafisi, "Overarching sustainable energy management of PV integrated EV parking lots in reconfigurable microgrids using generative adversarial networks," *IEEE Trans. Intell. Transp. Syst.*, vol. 23, no. 10, pp. 19258–19271, Oct. 2022.

[14] I. N. Moghaddam, B. Chowdhury, and M. Doostan, "Optimal sizing and operation of battery energy storage systems connected to wind farms participating in electricity markets," *IEEE Trans. Sustain. Energy*, vol. 10, no. 3, pp. 1184–1193, Jul. 2019.

[15] S. Nazari, F. Borrelli, and A. Stefanopoulou, "Electric vehicles for smart buildings: A survey on applications, energy management methods, and battery degradation," *Proc. IEEE*, vol. 109, no. 6, pp. 1128–1144, Dec. 2020.

[16] A. Aitio and D. A. Howey, "Predicting battery end of life from solar off-grid system field data using machine learning," *Joule*, vol. 5, no. 12, pp. 3204–3220, Dec. 2021.

[17] J. Tian, R. Xiong, W. Shen, and F. Sun, "Electrode ageing estimation and open circuit voltage reconstruction for lithium ion batteries," *Energy Storage Mater.*, vol. 37, pp. 283–295, May 2021.

[18] B. Pang, L. Chen, and Z. Dong, "Data-driven degradation modeling and SOH prediction of Li-ion batteries," *Energies*, vol. 15, no. 15, p. 5580, Aug. 2022.

[19] D. N. How, M. A. Hannan, M. H. Lipu, and P. J. Ker, "State of charge estimation for lithium-ion batteries using model-based and data-driven methods: A review," *IEEE Access*, vol. 7, pp. 136116–136136, 2019.

[20] L. Lam and P. Bauer, "Practical capacity fading model for Li-ion battery cells in electric vehicles," *IEEE Trans. Power Electron.*, vol. 28, no. 12, pp. 5910–5918, Dec. 2013.

[21] Y. Zhou and M. Huang, "Lithium-ion batteries remaining useful life prediction based on a mixture of empirical mode decomposition and ARIMA model," *Microelectron. Rel.*, vol. 65, pp. 265–273, Oct. 2016.

[22] K. Liu, Y. Shang, Q. Ouyang, and W. D. Widanage, "A data-driven approach with uncertainty quantification for predicting future capacities and remaining useful life of lithium-ion battery," *IEEE Trans. Ind. Electron.*, vol. 68, no. 4, pp. 3170–3180, Apr. 2021.

[23] J. Han and M. van der Baan, "Empirical mode decomposition for seismic time-frequency analysis," *Geophysics*, vol. 78, no. 2, pp. O9–O19, Mar. 2013.

[24] B. Xu, A. Oudalov, A. Ulbig, G. Andersson, and D. S. Kirschen, "Modeling of lithium-ion battery degradation for cell life assessment," *IEEE Trans. Smart Grid*, vol. 9, no. 2, pp. 1131–1140, Mar. 2018.

[25] M. Ghorbanzadeh, M. Astaneh, and F. Golzar, "Long-term degradation based analysis for lithium-ion batteries in off-grid wind-battery renewable energy systems," *Energy*, vol. 166, pp. 1194–1206, Jan. 2019.

[26] J. Li, L. Wang, C. Lyu, and M. Pecht, "State of charge estimation based on a simplified electrochemical model for a single LiCoO2 battery and battery pack," *Energy*, vol. 133, pp. 572–583, Aug. 2017.

[27] I. Laresgoiti, S. Käbitz, M. Ecker, and D. U. Sauer, "Modeling mechanical degradation in lithium ion batteries during cycling: Solid electrolyte interphase fracture," *J. Power Sources*, vol. 300, pp. 112–122, Dec. 2015.

[28] H. Farzin, M. Fotuhi-Firuzabad, and M. Moeini-Aghtaie, "A practical scheme to involve degradation cost of lithium-ion batteries in vehicle-to-grid applications," *IEEE Trans. Sustain. Energy*, vol. 7, no. 4, pp. 1730–1738, Oct. 2016.

[29] M. Swierczynski, D. I. Stroe, A. I. Stan, R. Teodorescu, and S. K. Kær, "Lifetime estimation of the nanophosphate $LiFeP_4$/C battery chemistry used in fully electric vehicles," *IEEE Trans. Ind. Appl.*, vol. 51, no. 4, pp. 3453–3461, Jul. 2015.

[30] W. Vermeer, G. R. C. Mouli, and P. Bauer, "A comprehensive review on the characteristics and modelling of lithium-ion battery ageing," *IEEE Trans. Transport. Electrific.*, vol. 8, no. 2, pp. 2205–2232, Jun. 2022.

[31] X. Ke, N. Lu, and C. Jin, "Control and size energy storage systems for managing energy imbalance of variable generation resources," *IEEE Trans. Sustain. Energy*, vol. 6, no. 1, pp. 70–78, Jan. 2015.

[32] M. Sandelic, A. Sangwongwanich, and F. Blaabjerg, "Incremental degradation estimation method for online assessment of battery operation cost," *IEEE Trans. Power Electron.*, vol. 37, no. 10, pp. 11497–11501, Oct. 2022.

[33] Y. Shi, B. Xu, Y. Tan, D. Kirschen, and B. Zhang, "Optimal battery control under cycle aging mechanisms in pay for performance settings," *IEEE Trans. Autom. Control*, vol. 64, no. 6, pp. 2324–2339, Jun. 2019.

[34] R. Khorram-Nia, B. Bahmani-Firouzi, and M. Simab, "Optimal scheduling of reconfigurable microgrids incorporating the PEVs and uncertainty effects," *IET Renew. Power Gener.*, vol. 2022, pp. 1–13, Jan. 2022.

[35] P. Li, L. Song, J. Qu, Y. Huang, X. Wu, X. Lu, and S. Xia, "A two-stage distributionally robust optimization model for wind farms and storage units jointly operated power systems," *IEEE Access*, vol. 9, pp. 111132–111142, 2021.

[36] J.-O. Lee, Y.-S. Kim, T.-H. Kim, and S.-I. Moon, "Novel droop control of battery energy storage systems based on battery degradation cost in islanded DC microgrids," *IEEE Access*, vol. 8, pp. 119337–119345, 2020.

[37] L. Zhang, Y. Yu, B. Li, X. Qian, S. Zhang, X. Wang, X. Zhang, and M. Chen, "Improved cycle aging cost model for battery energy storage systems considering more accurate battery life degradation," *IEEE Access*, vol. 10, pp. 297–307, 2022.

[38] M. Amini, A. Khorsandi, B. Vahidi, S. H. Hosseinian, and A. Malakmahmoudi, "Optimal sizing of battery energy storage in a microgrid considering capacity degradation and replacement year," *Electr. Power Syst. Res.*, vol. 195, Jun. 2021, Art. no. 107170.

[39] K. Ginigeme and Z. Wang, "Distributed optimal vehicle-to-grid approaches with consideration of battery degradation cost under real-time pricing," *IEEE Access*, vol. 8, pp. 5225–5235, 2020.
[40] G. Abdelaal, M. I. Gilany, M. Elshahed, H. M. Sharaf, and A. El'gharably, "Integration of electric vehicles in home energy management considering urgent charging and battery degradation," *IEEE Access*, vol. 9, pp. 47713–47730, 2021.
[41] A. S. Abdelaal, S. Mukhopadhyay, and H. Rehman, "Battery energy management techniques for an electric vehicle traction system," *IEEE Access*, vol. 10, pp. 84015–84037, 2022.
[42] D.-I. Stroe, M. Swierczynski, A.-I. Stroe, R. Laerke, P. C. Kjaer, and R. Teodorescu, "Degradation behavior of lithium-ion batteries based on lifetime models and field measured frequency regulation mission profile," *IEEE Trans. Ind. Appl.*, vol. 52, no. 6, pp. 5009–5018, Nov. 2016.
[43] D. E. Olivares, A. Mehrizi-Sani, A. H. Etemadi, C. A. Cañizares, R. Iravani, M. Kazerani, A. H. Hajimiragha, O. Gomis-Bellmunt, M. Saeedifard, R. Palma-Behnke, G. A. Jiménez-Estévez, and N. D. Hatziargyriou, "Trends in microgrid control," *IEEE Trans. Smart Grid*, vol. 5, no. 4, pp. 1905–1919, Jul. 2007.
[44] E. F. Camacho and C. B. Alba, *Model Predictive Control*. London, U.K.: Springer-Verlag, 2007.
[45] H. Farzin, M. Fotuhi-Firuzabad, and M. Moeini-Aghtaie, "Enhancing power system resilience through hierarchical outage management in multi-microgrids," *IEEE Trans. Smart Grid*, vol. 7, no. 6, pp. 2869–2879, Nov. 2016.
[46] *Sotavento Wind Farm*. Accessed: Jun. 1, 2021. [Online]. Available: http://www.sotaventogalicia.com/en/technical-area/realtimedata/historical/

MOHAMMAD AMINI received the B.Sc. degree in electrical engineering from the Isfahan University of Technology (IUT), Isfahan, Iran, in 2018, and the M.Sc. degree (Hons.) in electrical engineering from the Amirkabir University of Technology (Tehran Polytechnic), Tehran, Iran, in 2021. His current research interests include battery energy storage systems, smart grids, power systems optimization, and energy management systems. He has been a member of the Iran's National Elites Foundation (INEF), since 2021.

MOHAMMAD HASSAN NAZARI received the master's degree in power electrical engineering from the Sharif University of Technology, in 2013, and the Ph.D. degree in power system management from Tehran Polytechnic, in 2020. Since 2020, he has been a Postdoctoral Researcher with the Amirkabir University of Technology, where he has been an Associate Researcher, since 2022. His main research interests include integration of renewable energy sources, energy management systems, energy economic, power system resilience assessments, and distribution system planning and operation.

SEYED HOSSEIN HOSSEINIAN received the M.Sc. degree from the Amirkabir University of Technology (AUT), Tehran, Iran, in 1990, and the Ph.D. degree in electrical engineering from The University of Newcastle, Newcastle upon Tyne, U.K., in 1995. He is currently a Professor with the Department of Electrical Engineering, AUT. His research interests include transient in power systems, power quality, power system management, restructuring, and deregulation in power systems.